Chemico-Biological Interactions 351 (2022) 109728

Contents lists available at ScienceDirect

Chemico-Biological Interactions

journal homepage: www.elsevier.com/locate/chembioint

The hepatocyte export carrier inhibition assay improves the separation of hepatotoxic from non-hepatotoxic compounds

Tim Brecklinghaus [a,*,1], Wiebke Albrecht [a,1], Franziska Kappenberg [b,1], Julia Duda [b], Nachiket Vartak [a], Karolina Edlund [a], Rosemarie Marchan [a], Ahmed Ghallab [a,c], Cristina Cadenas [a], Georgia Günther [a], Marcel Leist [d], Mian Zhang [e], Iain Gardner [e], Jörg Reinders [a], Frans GM. Russel [f], Alison J. Foster [g], Dominic P. Williams [g], Amruta Damle-Vartak [a,h], Melanie Grandits [i], Gerhard Ecker [i], Naim Kittana [j], Jörg Rahnenführer [b,2], Jan G. Hengstler [a,2,*]

[a] Leibniz Research Centre for Working Environment and Human Factors at the Technical University of Dortmund (IfADo), Ardeystrasse 67, 44139, Dortmund, Germany
[b] Department of Statistics, TU Dortmund University, Vogelpothsweg 87, 44227, Dortmund, Germany
[c] Department of Forensic Medicine and Toxicology, Faculty of Veterinary Medicine, South Valley University, 83523, Qena, Egypt
[d] In Vitro Toxicology and Biomedicine, Department of Biology, University of Konstanz, Universitätsstr. 10, PO Box M657, 78457, Constance, Germany
[e] Simcyp (A Certara Company), Sheffield, UK
[f] Department of Pharmacology and Toxicology, Radboud University Medical Center, Nijmegen, the Netherlands
[g] Clinical Pharmacology and Safety Sciences, R&D, AstraZeneca, Cambridge, United Kingdom
[h] Division of Signal Transduction and Growth Control, DKFZ-ZMBH Alliance, German Cancer Research Center (DKFZ), 69120, Heidelberg, Germany
[i] University of Vienna, Department of Pharmaceutical Sciences, Althanstraße 14, Vienna, Austria
[j] Department of Biomedical Sciences, Faculty of Medicine and Health Sciences, An-Najah National University, PO Box 7, Nablus, Palestine

ARTICLE INFO

Keywords:
Cholestasis
DILI
Transport

ABSTRACT

An in vitro/in silico method that determines the risk of human drug induced liver injury in relation to oral doses and blood concentrations of drugs was recently introduced. This method utilizes information on the maximal blood concentration (C_{max}) for a specific dose of a test compound, which can be estimated using physiologically-based pharmacokinetic modelling, and a cytotoxicity test in cultured human hepatocytes. In the present study, we analyzed if the addition of an assay that measures the inhibition of bile acid export carriers, like BSEP and/or MRP2, to the existing method improves the differentiation of hepatotoxic and non-hepatotoxic compounds. Therefore, an export assay for 5-chloromethylfluorescein diacetate (CMFDA) was established. We tested 36 compounds in a concentration-dependent manner for which the risk of hepatotoxicity for specific oral doses and the capacity to inhibit hepatocyte export carriers are known. Compared to the CTB cytotoxicity test, substantially lower EC_{10} values were obtained using the CMFDA assay for several known BSEP and/or MRP2 inhibitors. To quantify if the addition of the CMFDA assay to our test system improves the overall separation of hepatotoxic from non-hepatotoxic compounds, the toxicity separation index (TSI) was calculated. We obtained a better TSI using the lower alert concentration from either the CMFDA or the CTB test (TSI: 0.886) compared to considering the CTB test alone (TSI: 0.775). In conclusion, the data show that integration of the CMFDA assay with an in vitro test battery improves the differentiation of hepatotoxic and non-hepatotoxic compounds in a set of compounds that includes bile acid export carrier inhibitors.

* Corresponding authors. IfADo, Ardeystrasse 67, 44139 Dortmund, Germany.
E-mail addresses: brecklinghaus@ifado.de (T. Brecklinghaus), hengstler@ifado.de (J.G. Hengstler).
[1] Shared first authorship.
[2] Shared senior authorship.

https://doi.org/10.1016/j.cbi.2021.109728
Received 23 June 2021; Received in revised form 15 October 2021; Accepted 25 October 2021
Available online 27 October 2021

Abbreviations

5-CMF	5-Chloromethylfluorescein
BC	Brain-Cousens
BSEP	Bile salt export pump
BSO	DL-buthionine sulfoximine
C_{max}	Maximal blood concentration
CMFDA	5-Chloromethylfluorescein diacetate
CTB	Cell-Titer Blue
DILI	Drug-induced liver injury
EC	Effective concentration
GSH	Reduced glutathione
GSSG	Oxidized glutathione
ML	Monolayer
MRP2	Multidrug resistance-associated protein 2
PHH	Primary human hepatocytes
SC	Sandwich
SOP	Standard operating procedure
TBHQ	tert-Butylhydroquinone
TEI	Toxicity estimation index
TSI	Toxicity separation index

1. Introduction

Prediction of drug-induced liver injury (DILI) remains a major challenge [1–3]. Recently, an in vitro/in silico method was established that determines the risk of human DILI in relation to oral doses and blood concentrations of a test compound [4]. An advantage of the published procedure is that it also allows for the optimization of an in vitro test system by calculating two novel metrics - the toxicity estimation index (TEI) and toxicity separation index (TSI) - where the former determines how well hepatotoxic blood concentrations in vivo can be estimated for hepatotoxic compounds, and the latter determines the degree of separation of hepatotoxic from non-hepatotoxic test substances. These metrics are calculated for a specified set of test compounds based on i) the concentration where cytotoxicity in cultured human hepatocytes first becomes evident, and ii) the maximal blood concentration (C_{max}) of a dose of interest obtained by pharmacokinetic modeling. After adding a new readout to an existing test system, TEI and TSI would then be re-calculated to indicate if the addition improved performance. For instance, we previously demonstrated that considering the expression of a set of toxicity indicator genes in addition to cytotoxicity to determine the lowest in vitro alert concentration resulted in a better TEI than cytotoxicity alone [4].

Hepatotoxicity may be due to actions of drugs that lead to direct forms of cell death that proceed in similar ways in vitro and in vivo. Hepatocyte death is a key event in many types of human hepatotoxicity [5,6]. Therefore, several previous studies, including our own, used cytotoxicity of cultured hepatocytes as a readout to determine hepatotoxicity in humans [1,4,7]. A second type of adverse effects affects functional properties of hepatocytes without immediate fully cytotoxic consequences, e.g. altered gene expression, protein synthesis or transport capacities. In vivo, such effects may eventually lead to DILI and loss of hepatocytes. This may involve long exposure, combination with other stressful events or functional demands, or interaction with other cell types and body constituents. This second type of adverse effects would likely not be captured by cytotoxicity assays in resting, fully homeostatic hepatocytes. To capture such adverse drug effects, assays that detect functional impairment or changes of the cellular phenotype, e.g. the release of cytokines that may activate immune cells or myofibroblasts; or altered metabolic functions [8]; covalent binding of metabolites to proteins, need to be introduced in an in vitro test battery predicting DILI.

Many hepatotoxic compounds inhibit bile acid export carriers, such as bile salt export pump (BSEP) and multidrug resistance-associated protein 2 (MRP2), leading to an intracellular accumulation of bile acids and compromised hepatocellular functions [9]. Such an accumulation of bile acids may ultimately cause hepatocyte death and is consequently detectable using cytotoxicity assays. However, it is unknown if using cytotoxicity as a single readout is sufficient to achieve an optimal differentiation of hepatotoxic and non-hepatotoxic compounds, or if a higher TSI can be obtained when carrier inhibition is included as an additional readout. To address this, we used the fluorescein export assay (CMFDA assay). In this assay, cells are treated with the membrane-permeable, non-fluorescent compound, 5-chloromethylfluorescein diacetate (CMFDA), which is catalyzed to fluorescent 5-chloromethylfluorescein (5-CMF) upon entering the cell by non-specific cytosolic esterases (Fig. 1). Importantly, 5-CMF is unable to cross the cell membrane, but instead can be actively exported by membrane transporters, such as BSEP and MRP2, either on its own or conjugated to GSH [10]. Consequently, the CMFDA assay can be used to investigate export inhibition by test compounds by detecting the delayed clearance of 5-CMF-associated green fluorescence from hepatocytes, or the delayed increase in fluorescence in the culture medium.

In the present study, we optimized the CMFDA assay and tested a set of hepatotoxic compounds known to inhibit BSEP and/or MRP2 in comparison to non-hepatotoxic compounds.

2. Materials and methods

2.1. Chemicals

An overview of the test compounds, tested concentration ranges, hepatotoxicity in humans and carrier inhibition data of the test compounds is given in Supplement 1.

2.2. Primary human hepatocytes

Cryopreserved primary human hepatocytes (PHH) were purchased from BioIVT and Lonza. The donor characteristics are given in Supplement 1. PHH were cultured according to a published standard operating procedure (SOP) ([11] supplement 2). Briefly, PHH were thawed and diluted with phenol red free William's E media (PAN-Biotech, Aidenbach, Germany) supplemented with 2 mM glutamine (PAN-Biotech, Aidenbach, Germany), 100 nM dexamethasone (Sigma Aldrich, Darmstadt, Germany), 2 ng/ml Insulin-Transferrin-Selenium (ITS), (Sigma Aldrich, Darmstadt, Germany), 100 U/ml penicillin and 0.1 mg/ml streptomycin (PAN-Biotech, Aidenbach, Germany), 10 μg/ml gentamicin (PAN-Biotech, Aidenbach, Germany) and 10% (v/v) SeraPlus (PAN-Biotech, Aidenbach, Germany). After counting and diluting, 50,000 viable cells were seeded in black 96-well plates (Greiner Bio-One, Kremsmünster, Austria) on a collagen monolayer. To avoid edge effects the outer wells were filled with culture medium only. After 3–4 h of attachment, the medium was changed to serum free William's E medium with the aforementioned supplements and cells were cultured under standard cell culture conditions (37 °C in a humidified atmosphere with 5% CO_2).

2.3. Compound treatment and CTB test

Compound treatment and testing for mitochondrial function (which usually correlates well to cytotoxicity) was performed by the CellTiter

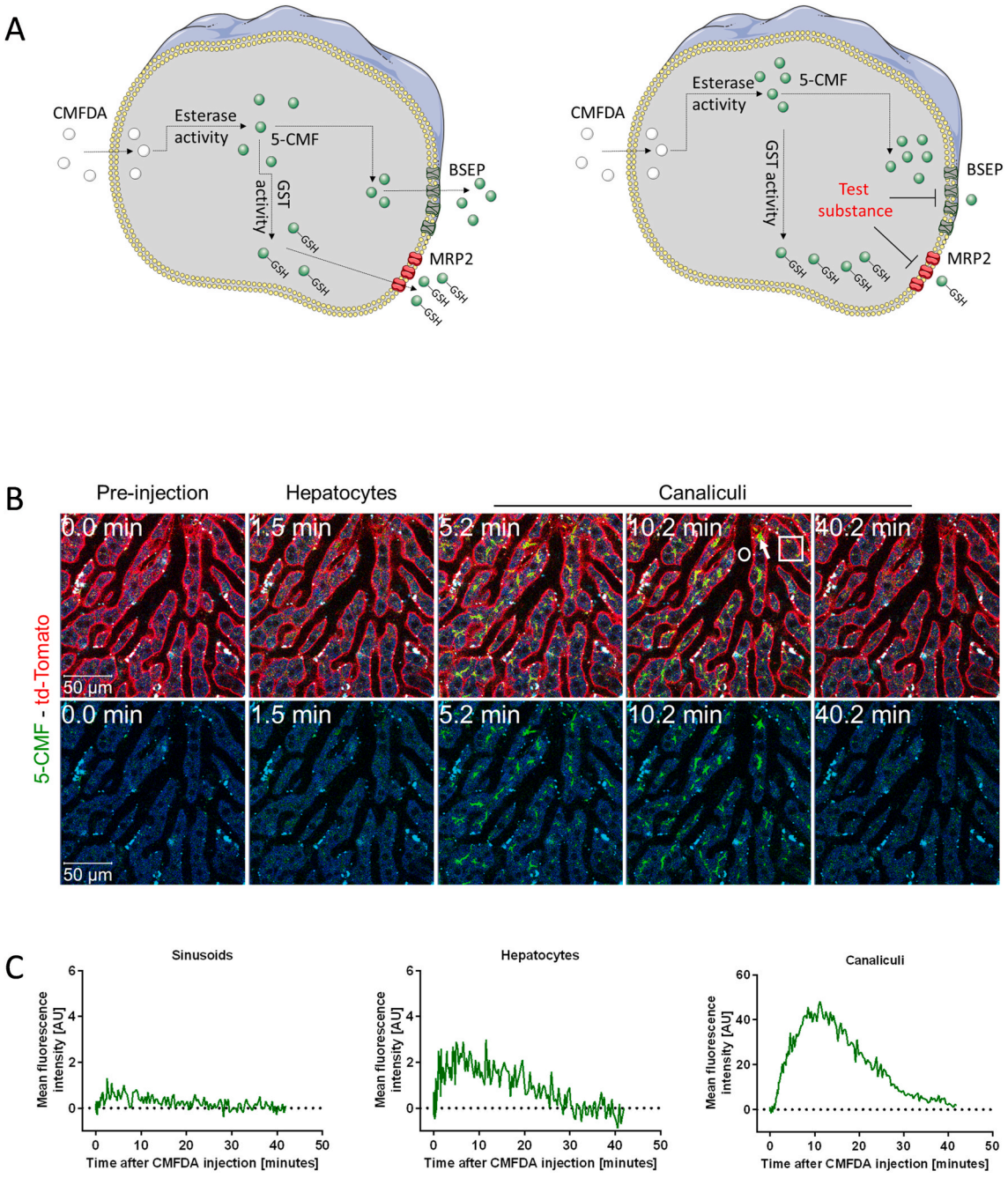

Fig. 1. Secretion of small molecules by hepatocytes. A. Principle of the CMFDA assay. 5-chloromethylfluorescein diacetate (CMFDA) freely passes through cell membranes into the cytoplasm, where it is transformed to the highly fluorescent 5-chloromethylfluorescein (5-CMF) by esterases. 5-CMF is actively exported by BSEP or MRP2 either as parent compound or after conjugation with glutathione (GSH). Therefore, inhibitors of BSEP or MRP2 increase intracellular fluorescence while extracellular concentrations of 5-CMF or its GSH conjugate decrease. Graphical elements were taken from Servier Medical Art by Servier. **B.** Stills of intravital two-photon imaging of 5-CMF secretion by mouse hepatocytes into bile canaliculi after tail vein injection of CMFDA. Green fluorescence occurs initially in the cytoplasm of hepatocytes and subsequently is enriched in bile canaliculi. The corresponding video is available in the supplement (Video 1). **C.** Quantification of 5-CMF associated fluorescence in the indicated regions of interest. Circle: sinusoid; square: hepatocyte; arrow: bile canaliculus. Time after injection of CMFDA is given in the upper left corner of the panels. Td-tomato: membrane targeted tandem dimer tomato sequence that expresses red fluorescence on the cell membrane. The upper panel shows the merged image of the td-tomato (red) and the 5-CMF (green) associated fluorescence, the lower panel only the green signal of 5-CMF.

Blue (CTB) assay as described [11]. In brief, 16–20 h after seeding, the cells were incubated with the indicated concentrations of the corresponding test compounds for 48 h. After incubation, the cells were washed three times and the CellTiter-Blue® Cell Viability Assay (Promega, Madison, Wisconsin, USA) was performed. The CTB assay was performed in hepatocytes of at least 3 different human donors each with 3–4 technical replicates.

2.4. CMFDA assay

For a detailed standard operating procedure (SOP) see Supplement 2. In brief, the day after seeding, cells were incubated for 1 h with the corresponding compound of interest followed by 20 min incubation with 2 μM CMFDA. Afterwards, the supernatant was transferred into a black 96-well plate (Greiner Bio-One, Kremsmünster, Austria) and fluorescence was measured with a Tecan Infinite 200 pro plate reader (Tecan Trading AG, Switzerland) at 485 nm excitation and 515 nm emission. The cells were washed three times with phosphate buffered saline (PBS), and fluorescence was measured with the settings mentioned before (485 nm excitation and 515 nm emission). The CMFDA assay was performed in hepatocytes of 3 different human donors each with 3 technical replicates. Raw data and processed data of the CMFDA assay are documented in Supplement 3.

2.5. Fluorescence microscopy of human hepatocytes

Live imaging. For the monolayer format, 200,000 cells were seeded in a 4-well IBIDI chamber (Ibidi, Gräfelfing, Germany) on a collagen monolayer as described before ([11] Supplement 2). For the sandwich format, 200,000 cells were seeded between two collagen layers (1 mg/ml). Here, 10 mg lyophilized rat-tail collagen was dissolved overnight in 9 ml 0.2% acetic acid at 4 °C. After the addition of 1 ml 10 × DMEM (BioConcept, Allschwil, Switzerland) and neutralization with 1 M NaOH, the IBIDI chamber was coated and incubated for 45 min at 37 °C and 5% CO_2. Upon seeding and attachment, the cells were washed, and the second collagen layer was added and incubated for a further 30 min at 37 °C and 5% CO_2. Finally, cultivation medium was added. The day after seeding, cells were acclimatized in the climate-control chamber at 37 °C and 5% CO_2, images were taken on a Zeiss LSM880 confocal microscope (Zeiss, Oberkochen, Germany). Image acquisition was performed with a 488 nm Argon laser, emission bands set to 503–558 nm. Pictures were taken before and after the treatment with 2 μM CMFDA.

Fixed cells. To detect the localization of BSEP in monolayer cultured hepatocytes, 200,000 cells were seeded in a 4-well IBIDI chamber (Ibidi, Gräfelfing, Germany) on a collagen monolayer as described before ([11] Supplement 2). The day after seeding, the cells were fixed and stained with the primary polyclonal rabbit antibody PA5-78690 (dilution: 1:200), the corresponding secondary polyclonal donkey anti-rabbit antibody A32790 (dilution: 1:200) and Hoechst 33342H3570 (dilution 1:8000) from Thermo Scientific. Images were taken on a Zeiss LSM880 confocal microscope (Zeiss, Oberkochen, Germany) using the manufacturer's provided software.

2.6. Cultivation and imaging of mouse hepatocytes

Mouse hepatocytes were isolated using a published standard operating procedure (SOP) [2]. Hepatocytes from tdTomato mice (Gt(ROSA)26Sortm14(CAG-tdTomato)Hze, Jackson lab, male, 8–12 weeks old) were used to establish spheroid and sandwich cultures. For spheroid cultures a previously described technique was used [12] with modifications. Briefly, 1,000 primary mouse hepatocytes per spheroid were cultured for 5 days in a hanging drop (Gravity ^{plus} culture format; InSphero, Schlieren, Switzerland). On day five after inoculation the microtissues were fixed in a collagen coated 35 mm, 1.5 coverslip and 14 mm glass diameter culture dish (MatTek, Ashland.MA). For the CMFDA uptake study the spheroid was exposed to 800 μl William's E medium containing a final concentration of 3.2 μM CMFDA. Images were acquired using a custom made inverted LSM 7 MP (Zeiss) with an LD C-Apochromat 40 × 1.1 water immersion objective and maintained at 37 °C and 5% CO_2 in an incubation chamber (Solent Scientific). For two-photon excitation, a Chameleon Ultra II laser (Coherent) tuned to 870 nm was used.

For sandwich cultures, the SOP published in Godoy et al. (2013) [2] was used. The hepatocytes were isolated from the same mouse strain (td tomato) and one million of primary mouse hepatocytes (td-tomato) were seeded on a Glass Bottom Culture Dish (MatTek) precoated with a first layer of 200 μl collagen (250 μg/ml rat tail collagen I cell culture grade Roche). Three hours after attachment, the cells were washed and 250 μl of the second layer was added. After the cells were cultured for three days, the culture medium was removed and 800 μl fresh William's medium with 0.05 mM Hoechst dye [13] was added. CMFDA at a final concentration of 1.6 μM in the culture medium was repeatedly added. Images were acquired by the same microscope (LSM 7 MP) as for spheroid cultures.

2.7. GSH analysis

To obtain further insight into the mechanism and to clarify if the thiol concentration influences the CMFDA assay, primary human hepatocytes of three different donors were incubated for 48 h with DL-buthionine sulfoximine (BSO), a selective inhibitor of glutathione synthesis (Sigma Aldrich 19176-250 MG), and the antioxidant tert-butylhydroquinone (TBHQ) (Sigma Aldrich 112941-100G). Afterwards, the CTB and CMFDA assays were performed and total reduced glutathione (GSH) and oxidized glutathione (GSSG) were analyzed by mass spectrometry. Here, samples were derivatized using N-ethylmaleimide as described by New and Chan [14], followed by separation on a 3 × 150 mm Nucleodur PolarTec (3 μm) reversed phase column using a Vanquish Horizon UHPLC coupled online to a QExactive mass spectrometer (both ThermoFisher, Germany) operating in PRM-mode. Generated data were quantified using Skyline [15].

2.8. Transporter prediction

A publicly available web service was used that predicts if small molecules inhibit the export carriers BSEP, MRP3 and MRP4 of hepatocytes [16]. The web service predicts a binary outcome, indicating whether the query compound is active or not. Each transporter model is based on a different classifier and the structure of the molecules are described with RDKit descriptors. A detailed description of the models is given at https://livertox.univie.ac.at [16].

2.9. Intravital imaging of CMFDA clearance in mice in vivo

The intravital imaging of CMFDA clearance in the livers of mice was performed as described in a recently published protocol [13]. As described in this protocol, mT/mG reporter mice were applied and an inverted two-photon microscope LSM MP7 (Zeiss, Jena, Germany) with an LD C-Apochromat 40 × 1.1 water immersion objective was used [13,17]. A bolus of 20 μg CMFDA (Thermo Scientific, MA, USA; Cat. No. C7025) was intravenously administered using a tail vein catheter (SAI-infusion, IL, USA). Quantification of mean fluorescence intensity of 5-CMF in the hepatic sinusoids, hepatocytes, and bile canaliculi was done in a specified region of interest using ZEN software (Zeiss, Jena, Germany) as indicated in the corresponding figures. All experiments were approved by the local animal protection agency. Animal experiments were approved by the local authorities, husbandry was performed as per the German Animal Welfare Act (1972), Animal Protection Laboratory Animal Regulations (2013), and European Directive 2010/63/EU.

2.10. Statistical analysis

All statistical analyses were performed with R, version 4.0.0 [18], using the R-packages *DoseFinding,* version 0.9–17 [19] and *drc,* version 3.0–1 [20]. The R package *pROC* was used to calculate the TSI [21].

2.10.1. Curve fitting and calculation of EC values

For the CTB test, the processing of the raw data, curve fitting, calculation of the GoF (goodness-of-fit), and estimation of EC values was performed as previously described [4,22]. First, three models were fitted to the data of each compound, including i) a four-parameter log-logistic model (4pLL), ii) a Brain-Cousens (BC) model [23], and iii) a flat profile. The parametric functions for the logistic-type 4pLL model with sigmoidal shape and for the Brain-Cousens model with an additional parameter specifying a potential hormesis effect are given in Supplement 4A. A flat profile means that no relevant changes occurred in the CTB test with respect to the test compound concentrations. In this case a constant, calculated as the mean viability across all concentrations, was fitted to the CTB test data. Then, the Akaike Information Criterion (AIC) [24] was calculated for each model, and the model with lowest AIC value was selected for final normalization and curve fitting. If the flat profile was chosen, data was normalized such that the curve attains the value 100% (i.e. the mean was transformed to 100%). Normalization of the 4pLL and the BC model and estimation of the EC values for the BC model was conducted as described before [22], with the exception that the normalization of the BC model was performed with respect to the left asymptote instead of the maximum value. EC values were only calculated for curves where the mean response value at the concentration $conc_{\max}$ (the highest tested concentration of the respective compound) was smaller than 90% after normalization and the value of the GoF was larger than 0.55. The other (missing) EC values were replaced with the value $conc_{\max} \times 5$, so called penalty. EC values for compounds were calculated using the minimum, median and maximum across all donors. When cryopreserved hepatocytes of individual donors were assessed twice, both resulting EC values were included with weight 0.5 for the calculation of the minimum, median and maximum across all donors. For a detailed overview of the raw and processed data, see Supplement 3.

For the export inhibition data (CMFDA assay), the raw data were processed as follows: Replicates of the control values were averaged for each biological replicate separately. Fluorescence values of all replicates were divided by the corresponding averaged control values and multiplied by 100 to obtain percentages. Since the shapes of the curves of the CMFDA assay differed from the shapes of the CTB test, they were instead fitted using MCP-Mod (Multiple Comparison Procedure and Modeling), a two-step modelling approach that considers model uncertainty [25]. Based on MCP, each concentration-response curve was evaluated with respect to the compound effect, considering candidate curves as illustrated in Supplement 4B. For the set of candidate curves, a multivariate two-sided contrast *t*-test tailored to the shapes of the candidate curves was calculated for each concentration-response data set at a family wise error rate of $\alpha = 0.05$ to adjust for multiple testing. Either the test selected one model according to the AIC (in case p-value < 0.05) or, if no model was selected (in case p-value ≥ 0.05), a flat concentr ation-response profile was assumed indicated by a horizontal red line in the concentration response curves. In the Mod-step, the chosen model was fitted to the data. The MCP-Mod procedure was applied three times for each scenario of compound and donor, for (i) the measurements of the pre-processed cell data, (ii) the measurements of the supernatant data, and (iii) the difference of the measurements of the two ('data--difference'). For (iii), the measurements were matched by their concentration and technical replicate. The curves were shifted such that the response at concentration 0 is at 100% for (i) and (ii) and at 0% for (iii). EC_x values were calculated as the lowest concentration where the curve attains the response of (100+x)% for (i), (100-x)% for (ii), and x% for (iii). Additionally, a difference of the models ('model-difference') for (i) and (ii) was calculated, and corresponding EC_x values were obtained as for (iii). In subsequent analyses, the median EC_x values of the three biological replicates was used for each compound. Alternatively, the minimum and maximum was used. Only for the case where the CMFDA assay-based EC_x values were considered individually, missing values were replaced by $conc_{\max} \times 5$ (penalty). When analysing the combination of CMFDA assay-based EC_x values and CTB assay-based EC_x values, the compound-wise minimum was used and only the CTB assay-based values were replaced by $conc_{\max} \times 5$ (penalty) in the case of missing values. For a detailed overview of the raw and processed data, see Supplement 3.

2.10.2. Calculation of toxicity separation and estimation indices

The toxicity separation index (TSI) and toxicity estimation index (TEI) were calculated based on the in vitro alert concentration (e.g. EC_{10} of the CTB assay) and the in vivo value for the C_{max} for each test compound, as described in detail in Ref. [4]. In brief, TSI is determined by calculating the $\log_{10}$ difference between C_{max} and EC_{10} for all compounds, sorting the differences in ascending order, choosing a cutoff value in each interval between two consecutive differences, and for each cutoff value predicting the toxicity status of each compound. Comparing the predicted and the true toxicity status, the obtained sensitivity and 1-specificity is then plotted for each cutoff value and the TSI is calculated as the area under the ROC curve (AUC). Including only the hepatotoxic compounds, TEI is calculated as:

$$\mathrm{TEI} = 1 - \frac{1}{5} \frac{\sum_{i=1}^{n} 1_{toxic}(i) 1_{x(i)>y(i)} \left|\log_{10}\left(\frac{y(i)}{x(i)}\right)\right|}{\sum_{i=1}^{n} 1_{toxic}(i)}$$

where i = 1, …,n represent the compounds in question, x(i) and y(i) the in vitro value and the in vivo value of compound i, respectively, and $1_{(condition)}(i)$ the indicator function which takes the value 1 if the condition is fulfilled by the compound i, otherwise 0.

2.11. Simulation of pharmacokinetics

To calculate C_{max} for each test compound, a physiologically based pharmacokinetic (PBPK) model was constructed as described before [4] using the Simcyp Simulator (commercial software, Version 19; SimCyp, Sheffield, UK). All treatment regimens of the analyzed substances and input parameters of the pharmacokinetic simulations are given in Supplement 5. Certera UK (Simcyp Division) granted free access to the Simcyp Simulators through an academic licence (subject to conditions).

3. Results

3.1. Secretion of 5-CMF by spheroid and sandwich cultures in relation to the in vivo situation in mice

Hepatocytes can be cultured by different techniques, three-dimensional spherical cellular aggregates, further named spheroid cultures, or as sheets of cells that can either be cultured between two layers of collagen (sandwich cultures) or on a collagen coated dish, further referred to as monolayer. Since previous studies recommended the use of spheroids for in vitro tests, our first aim was to clarify if spheroid or sandwich cultures are more suited for the CMFDA assay. We began by comparing the secretion of 5-CMF from both in vitro models to the in vivo situation. For the in vivo analyses, we performed intravital imaging in mice due to the limitations of live imaging in humans, and later compared the results with those obtained from isolated mouse hepatocytes in order to establish the most appropriate experimental conditions for isolated human hepatocytes. To analyze hepatocyte secretion of 5-CMF in vivo, we applied a previously established two-photon microscopy technique in anaesthetized mice [6,13] using the mT/mG mouse

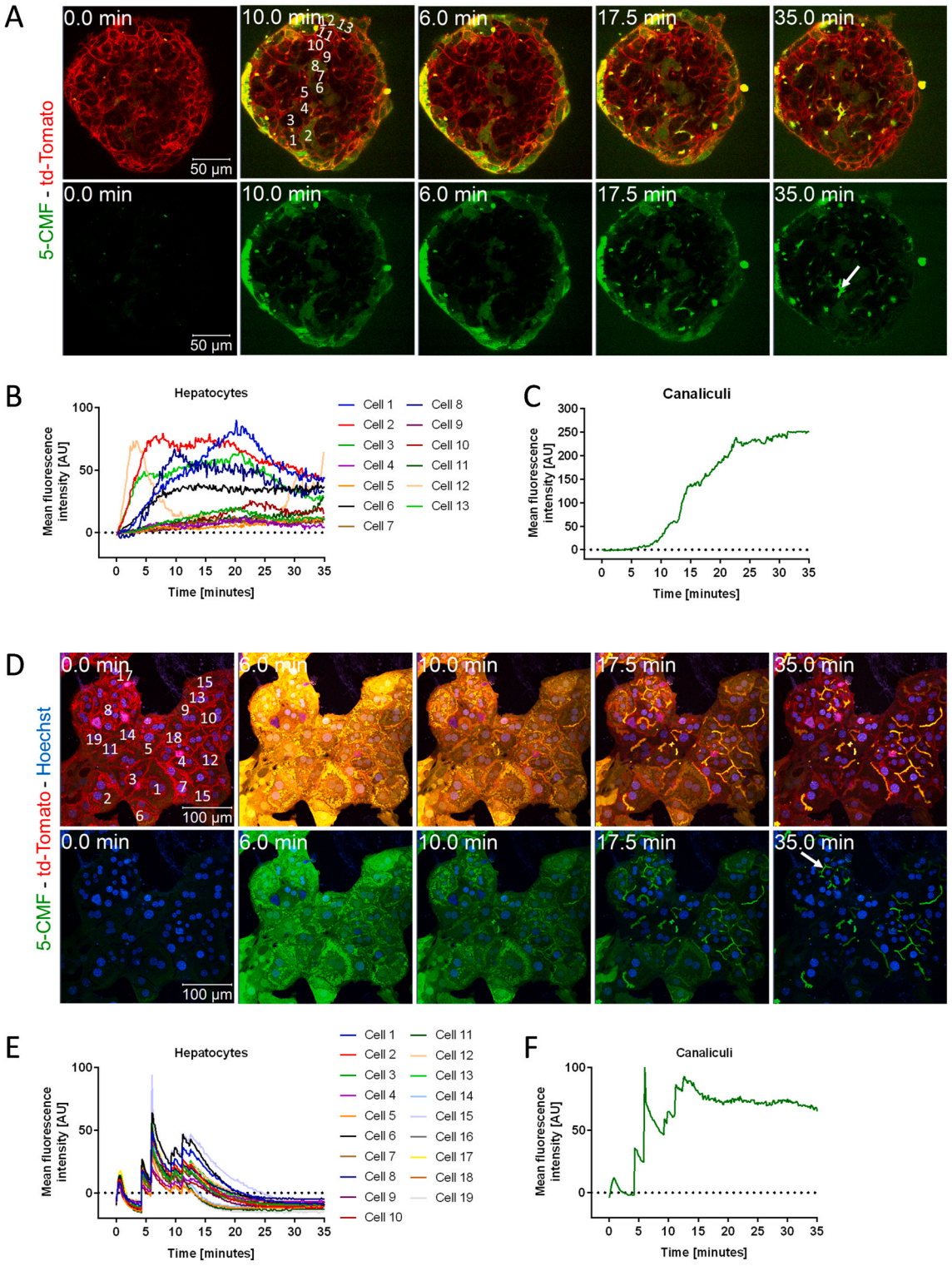

Fig. 2. Export of 5-CMF from cultured mouse hepatocytes. A–C: Spheroid cultures. **D–F:** Sheet (sandwich) cultures. **A.** Stills from an intravital video (Supplement: Video 2). The upper panel shows merged red and green fluorescence, the lower panel only the green signal. Time after addition of CMFDA is given in the upper left corner. The numbers in the spheroid (top panel, 2nd from left) indicate the regions of interest, where green fluorescence was quantified. **B.** Quantification of green fluorescence in the cells indicated by the numbers in A. **C.** Quantification of green fluorescence in the bile canaliculus indicated by the arrow in A (bottom right panel). **D.** Stills from a sandwich culture after repeated addition of CMFDA (four times) to the culture medium. The numbers indicate regions of interest, where green fluorescence was quantified. Quantification in hepatocytes **(E)** and a bile canaliculus **(F)**.

strain which has red fluorescence on all cell membranes due to a membrane-targeted tandem dimer tomato sequence [13]. After injection of CMFDA into the tail vein, 5-CMF associated green fluorescence transiently increased in hepatocytes, followed by enrichment in bile canaliculi (Fig. 1B and C; Video 1).

For the in vitro experiments, we used hepatocytes from the same mT/mG mouse strain, which allowed us to directly compare the 5-CMF export to that observed in vivo. Hepatocyte spheroids showed an increase in fluorescence (Fig. 2A and B; Video 2) followed by canalicular secretion (Fig. 2C). However, hepatocytes at the margin of the spheroid

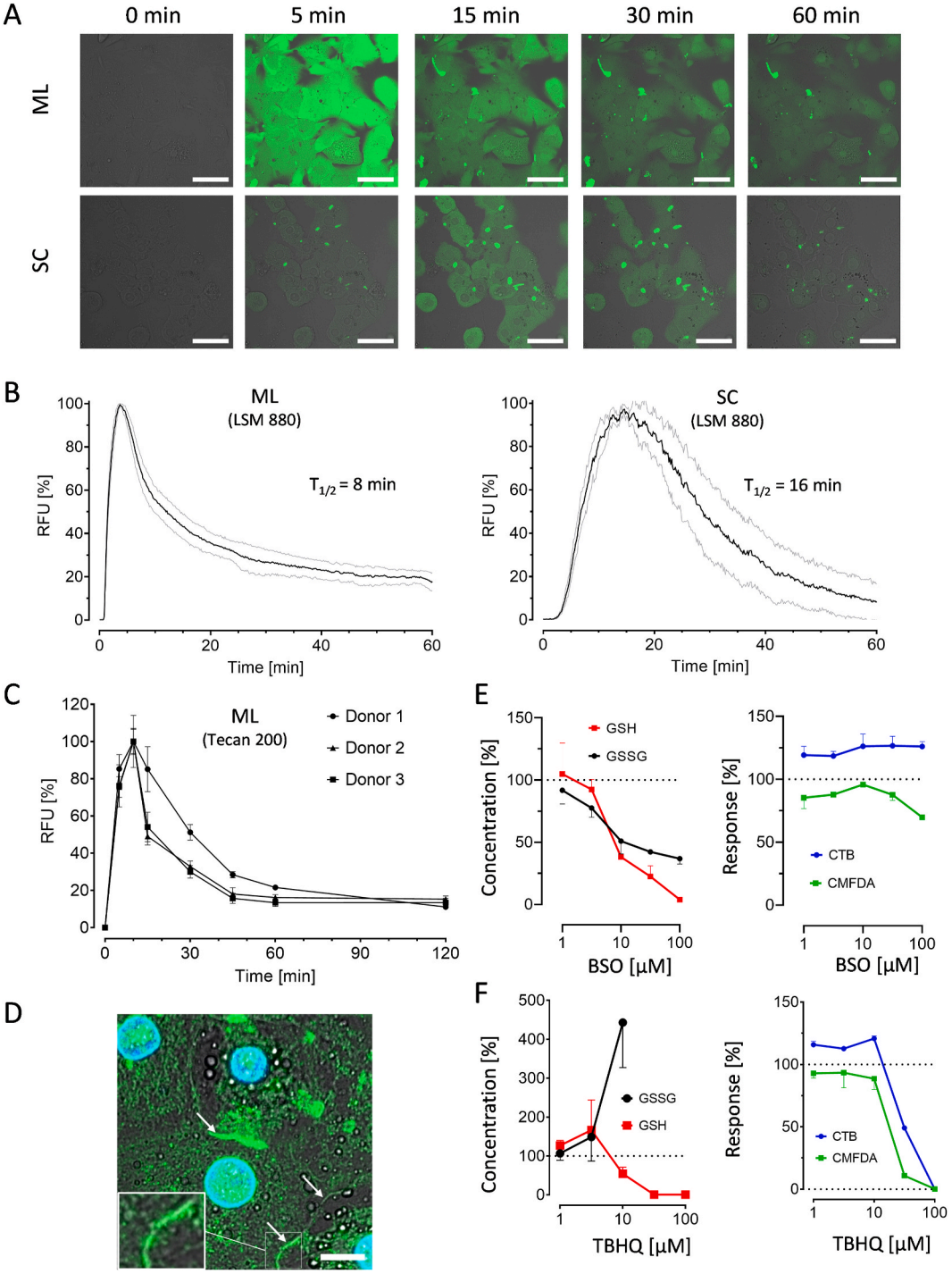

Fig. 3. Optimization of the CMFDA assay in human hepatocytes. A. Human hepatocytes cultured as collagen sandwiches (SC) or monolayer cultures (ML) in the presence of CMFDA. Scale bar: 50 µm. **B.** Fluorescence (excitation: 488; emission: 503–558) in SC and ML were detected by a laser scanning microscopy (LSM880). The three lines of the plots represent mean values and standard deviations (SD). **C.** Fluorescence of hepatocytes from three donors cultured as monolayers detected in a 96-well fluorescence reader. Data are given as mean ± SD. **D.** Visualization of the export transporter BSEP by immunostaining and confocal microscopy in monolayer cultured, cryopreserved human hepatocytes. Membrane localization is indicated by the white arrow. Blue: nuclear staining by Hoechst dye 33342. Scale bar: 10 µm. **E&F.** Cultured human hepatocytes (monolayers) were concentration-dependently incubated with BSO (E) or TBHQ (F) for 48 h. Intracellular concentrations of reduced (GSH) and oxidized (GSSH) glutathione, fluorescence of 5-CMF in hepatocytes after exposure to CMFDA, and the CTB test data are shown as mean ± SD. The two highest tested concentrations of TBHQ were cytotoxic and the concentrations of GSSG were below the detection limit (not shown in F).

showed a much stronger 5-CMF associated signal than cells at the center of the spheroid. Quantification of the time-fluorescence profile of 13 hepatocytes along the diameter of the spheroid demonstrated a large heterogeneity among hepatocytes (Fig. 2B), which hampers the establishment of a quantitative assay. In contrast, 5-CMF associated fluorescence was homogeneous among all 19 hepatocytes quantified in hepatocytes that were cultured as one cell layer between two layers of collagen (Fig. 2D–F; Video 3). Interestingly, adding CMFDA four times to the culture medium still led to a similar transient increase in green fluorescence in hepatocytes, supporting the suitability of this model for the export assay. In addition, excretion of 5-CMF occurred faster in the sandwich culture compared to the spheroid culture. Since homogeneity among hepatocytes is important for the establishment of automated quantification, and considering that in vivo hepatocytes are organized in sheets that rather resemble layers than spheroids along the blood sinusoids (Fig. 1B), we conducted all further experiments using hepatocytes cultured as sheets, i.e. as sandwich or monolayer cultures.

3.2. Excretion of 5-chloromethylfluorescein by human hepatocytes

Two different formats of human hepatocytes cultured as one sheet of hepatocytes were compared, the easy-to-handle monolayer where hepatocytes attach to collagen coated dishes (ML), and the more complex sandwich cultures, where hepatocytes are cultured between two layers of a collagen gel (SC). To compare the excretion kinetics of 5-CMF, cells were incubated with 2 μM CMFDA one day after seeding the cryopreserved human hepatocytes. Following the addition of CMFDA to the culture medium, the 5-CMF associated signal showed a transient increase in the cytoplasm of the hepatocytes for both ML and SC (Fig. 3A). For the ML, an increase in intracellular fluorescence was observed immediately after the addition of CMFDA (earliest time shown in Fig. 3A: 5 min), followed by a decrease in intracellular fluorescence; the bile canaliculi remained visible until the end of the imaging period (60 min). In contrast, it took 15–20 min before the maximum intracellular intensity was observed in the SC, probably because the layer of collagen gel delayed the passage of CMFDA to the hepatocytes. Nevertheless, the canaliculi were already visible at 5 min, most likely due to the high affinity of export carriers to 5-CMF that facilitated its enrichment in the canaliculi at already low intracellular concentrations present 5 min after the addition of CMFDA.

Quantification of cytoplasmic fluorescence over time confirmed that both the increase and decrease of cytoplasmic 5-CMF-associated fluorescence occurred earlier in ML than in SC (Fig. 3B). Moreover, the half-life of 5-CMF was shorter in ML (8 min) compared to SC (16 min). Thus, although both SC and ML successfully cleared 5-CMF from hepatocytes, supporting their suitability for the export inhibition assay, we nevertheless selected the monolayer culture for subsequent studies, primarily because they are easier to handle and standardize. A major challenge faced with using SC is the layer of collagen on top of the hepatocytes that influences clearance kinetics. Consequently, it is not sufficient to only standardize its thickness, but also to control the individual collagen gel batches with respect to their capacity to bind CMFDA and 5-CMF.

Since the assay was intended for a 96-well format using fluorescence measured with a spectrophotometer as the quantifiable endpoint, we next studied the reproducibility of the assay using hepatocytes from three donors plated in ML. Consistently, a peak of intracellular fluorescence was obtained at approximately 10 min after the addition of CMFDA followed by a decrease with relatively small inter-individual differences (Fig. 3C). Since the degree of clearance obtained with the 96-well fluorescence reader was similar to that observed with the confocal microscope (LSM 880), and the results were reproducible among the different donors, subsequent experiments were performed using the 96-well format.

Finally, previous studies performed using rodent hepatocytes reported a rapid loss of export carriers in monolayer cultures [26,27]. Therefore, we studied the expression of BSEP - one of the most critical export carriers - by immunostaining and confocal microscopy in monolayer cultures of human hepatocytes to confirm its presence at the cell membrane. We observed a relatively large fraction of BSEP in the cytoplasm and in cytoplasmic vesicles; however, the carrier was also located at the cell membrane (Fig. 3D), which corresponds to the observed export activity. This result may be explained by the choice of an early time-point (day 1 after seeding of the hepatocytes), prior to dedifferentiation of the hepatocytes. Moreover, human hepatocytes may dedifferentiate more slowly than those of rodents [2,3,26].

Based on these preliminary experiments, we defined all relevant experimental conditions in a standard operating procedure (SOP) (Supplement 2) with the following main steps: (1) Thawing and plating of cryopreserved hepatocytes on day −1; (2) test compound exposure for 1 h on day 0, followed by 20 min incubation with CMFDA (in the presence of test compound); (3) analysis of fluorescence in the cell culture supernatant; and (4) analysis of intracellular fluorescence after washing cells with PBS.

3.3. No influence of substances that deplete or induce glutathione levels

5-CMF is exported from hepatocytes as either itself or as a glutathione (GSH) conjugate (Fig. 1A), and to our knowledge, the export kinetics of either has not yet been quantified in human hepatocytes. In order to test the robustness of the assay, we investigated whether glutathione depletion or oxidation – relatively frequent mechanisms of hepatotoxic compounds, may influence the results. Thus, if 5-CMF and its GSH conjugate are exported by different rates, then compounds that alter cytoplasmic GSH levels, for example, by conjugating to GSH, may influence the results of the CMFDA assay. Therefore, we used two compounds that have been reported to alter intracellular GSH levels, DL-buthionine-sulfoximine (BSO), an inhibitor of gamma-glutamylcysteine synthetase [28], the rate limiting enzyme in GSH synthesis, and the NRF2 activator tert-butylhydroquinone (TBHQ) [29]. Incubations with BSO and TBHQ were performed for 48 h prior to the CMFDA assay. BSO reduced both GSH and GSSG (Fig. 3E), while TBHQ decreased GSH and increased GSSG (Fig. 3F). However, at non-cytotoxic concentrations neither BSO nor TBHQ influenced the results of the CMFDA assay (Fig. 3E; Fig. 3F; Supplement 6). Only at concentrations where mitochondrial function was compromised as evidenced by the CTB test (>10 μM), we observed a decrease in 5-CMF associated fluorescence. In conclusion, these experiments show that neither decreased intracellular glutathione levels with BSO nor GSH oxidation with TBHQ at non-cytotoxic test compound concentrations influenced the results of the CMFDA assay.

3.4. Analysis of test compounds by the CMFDA assay

We next analyzed different concentrations of 36 test compounds with the CMFDA assay using hepatocytes from at least three human donors (Table 1). The test compounds were chosen based on their known capacity to induce human hepatotoxicity and to inhibit BSEP and MRP2 (Supplement 1). An increased risk of human hepatotoxicity has been documented for 18 compounds based on a specific treatment regimen; whereas, 17 compounds are not known to cause an increased risk of hepatotoxicity (Supplement 5). Acetaminophen (APAP) was also included among the test compounds because of its dose-dependent hepatoxicity, i.e.- a C_{max} of up to 1.09×10^{-1} mM does not induce hepatotoxicity, while a C_{max} of 1.21 mM or higher is associated with an increased risk of human hepatotoxicity (Supplement 5). For the other selected compounds, it is not possible to make such a differentiation because information on whether the risk of hepatotoxicity increases with dose is only reliably documented for the therapeutic regimen. Twenty of the 36 test compounds are known to inhibit BSEP and/or MRP2 (Table 1; Supplement 1).

In principle, a test compound can interact with 5-CMF and alter its fluorescence which would compromise the results of the CMFDA assay.

Table 1
Summary of the results of the CTB tests, CMFDA assay and pharmacokinetic modeling of the test substances. All generated data including the raw data can be found in the supplement. Inhibition of hepatocellular carriers was indicated as "yes" if documented in at least one previous study together with an IC_{50}-value. "#" indicates that contradicting information has been reported, "N/A" indicates that no information could be identified.

Substance	Abbreviation	Hepatotoxicity reported	In vivo C_{max} whole blood 95% total [mM]	In vitro CTB test EC_{10} [mM] median [min/max]	In vitro CMFDA model-difference EC_{10} [mM] median [min/max]	Inhibition of hepatocellular export	
						BSEP	MRP2
Acetaminophen	APAP	no/yes	$1.09*10^{-01}$ $1.21*10^{+00}$	1.4027 [0.5000/2.8325]	>0.5 [>0.5/>0.5]	no	no
Atorvastatin	AVS	yes	$5.38*10^{-06}$	2.2384 [0.0742/>3.16]	>1 [>1/>1]	yes	yes
Atropine	ATRO	no	$1.50*10^{-05}$	0.1378 [0.0645/0.2076]	0.0009 [0.0006/0.0167]	no	yes
Benzbromarone	BZB	yes	$1.79*10^{-02}$	0.0102 [0.0095/0.0119]	0.0011 [0.0009/0.0014]	yes	yes
Benztropine	BZT	no	$1.23*10^{-05}$	0.0105 [0.0066/0.0382]	>0.5[>0.5/>0.5]	N/A	N/A
Bosentan	BOS	yes	$2.81*10^{-03}$	0.0175 [0.0033/0.0554]	0.0416 [0.0206/>0.1]	yes	no#
Chlorpheniramine	CHL	no	$6.49*10^{-05}$	0.0442 [0.0142/0.1550]	>0.5 [>0.5/>0.5]	no	no
Codeine	COD	no	$2.33*10^{-04}$	0.9564 [0.5363/1.0584]	>0.5 [>0.5/>0.5]	N/A	N/A
Cyclosporin A	CSA	yes	$7.34*10^{-03}$	0.0136 [0.0079/0.0308]	0.0006 [0.0004/0.0049]	yes	yes
Diphenhydramine	DPH	no	$5.90*10^{-04}$	0.1221 [0.0560/0.1426]	>0.5 [>0.5/>0.5]	no	no
Entacapone	ETC	yes	$9.94*10^{-03}$	0.019789 [0.0169/0.0342]	0.0049 [0.0025/0.0425]	yes#	no
Hydroxyzine	HYZ	no	$4.94*10^{-04}$	0.0788 [0.0447/0.0940]	0.0139 [0.0099/0.0358]	yes	N/A
Indomethacin	INDO	yes	$3.48*10^{-03}$	>0.2445 [0.0814/>0.2445]	0.0188 [0.0186/>0.1]	yes	yes#
Isosorbide dinitrate	ISS	no	$1.03*10^{-04}$	0.1078 [0.0975/0.1345]	>0.5 [>0.5/>0.5]	N/A	N/A
Ketoconazole	KC	yes	$1.62*10^{-02}$	0.0256 [0.0078/0.0998]	0.0027 [0.0019/0.0032]	yes	yes
Lovastatin	LO	yes	$8.48*10^{-06}$	>0.245 [0.0243/>0.245]	0.0167 [0.0097/>0.1]	yes	yes
Melatonin	MEL	no	$2.70*10^{-05}$	0.9208 [0.0767/>5]	>0.5 [0.4017/>0.5]	no	no
N-Acetylcysteine	NAC	no	$3.19*10^{-03}$	>10 [0.2425/>10]	>0.5 [>0.5/>0.5]	N/A	N/A
Nifedipine	NDP	yes	$1.16*10^{-03}$	>0.4328 [>0.4328/ >0.4328]	0.0029 [0.0001/0.0035]	yes	no
Oxycodone	OXC	no	$9.84*10^{-05}$	1.1488 [0.5456/6.3366]	>0.5 [0.0667/>0.5]	N/A	N/A
Oxymorphone	OXM	no	$1.13*10^{-05}$	0.0276 [0.0244/0.0432]	0.0330 [0.0029/>0.5]	N/A	N/A
Pazopanib	PZB	yes	$6.20*10^{-02}$	>0.189 [>0.189/>0.189]	>0.1 [0.0942/>0.1]	yes	no
Pindolol	PIN	no	$1.71*10^{-04}$	>0.5 [>0.5/>0.5]	>0.5 [>0.5/>0.5]	no	no
Pioglitazone	PIO	yes	$5.33*10^{-03}$	0.0085 [0.0077/0.0780]	>0.1 [0.0001/>0.1]	yes	no
Pyridoxine	PDX	no	$7.04*10^{-05}$	1.0227 [0.1055/5.0820]	>0.5 [0.4665/>0.5]	N/A	N/A
Rifampicin	RIF	yes	$2.01*10^{-02}$	0.2615 [0.1208/0.4241]	0.0040 [0.0025/0.0177]	yes	yes
Rosiglitazone	RGZ	yes	$5.99*10^{-04}$	0.0355 [0.0338/0.0472]	0.0275 [0.0162/>0.1]	yes	yes#
Rosuvastatin	ROS	yes	$9.78*10^{-06}$	0.0278 [0.0261/0.0279]	>0.1 [0.0029/>0.1]	yes	yes
Simvastatin	SIM	yes	$2.15*10^{-05}$	0.0196 [0.0133/0.0464]	0.0036 [0.0005/0.0056]	yes	yes
Sitaxentan	SXS	yes	$1.73*10^{-02}$	0.1317 [0.0861/0.1840]	0.0017 [0.0008/0.0024]	yes	yes#
4-Phenylbutyrate	SPB	no	$9.11*10^{-01}$	1.9690 [0.1919/>10]	>0.5 [>0.5/>0.5]	N/A	N/A
Theophylline	THE	no	$6.10*10^{-02}$	0.2138 [0.2046/0.9454]	>0.5 [0.0548/>0.5]	no	no
Tolcapone	TOLC	yes	$1.06*10^{-02}$	0.0281 [0.0200/0.0313]	0.0016 [0.0010/0.0063]	yes	no
Triprolidine	TPL	no	$3.16*10^{-05}$	0.1609 [0.1223/>1.6]	>0.5 [>0.5/>0.5]	yes	N/A
Troglitazone	TROG	yes	$2.21*10^{-03}$	0.0109 [0.0094/0.0222]	0.0009 [0.0006/0.0018]	yes	yes#
Zaleplon	ZAL	no	$1.94*10^{-04}$	0.0969 [0.0161/>0.5]	>0.5 [0.2684/>0.5]	no	no

To control for such effects, fluorescein was incubated with all test compounds using the concentration range of the CMFDA assay without the presence of cells (Supplement 8). None of the test compounds caused a change of the fluorescence intensity that exceeded 10%, demonstrating that interaction of the tested chemicals with the fluorophore did not compromise the results of the CMFDA assay.

To illustrate representative results of the CMFDA assay (Fig. 4A), two examples with expected positive (cyclosporine A and troglitazone) and two with expected negative results (chlorpheniramine and theophylline) are shown (Fig. 4B). Data from the complete set of compounds are available in Supplement 7. Cyclosporine A caused a concentration dependent increase in fluorescence in the hepatocytes, while the fluorescence signal decreased in the corresponding culture medium supernatants (Fig. 4B), a scenario that fits to the inhibition of 5-CMF export. However, fluorescence in the cell and in the supernatant were not just an inverse of each other, but rather the intracellular increase in signal occurred at lower concentrations compared to decreased extracellular fluorescence. The reasons for this deviation may be manifold, e.g. dilution of 5-CMF in the volume of the supernatant, or compound specific mechanisms not specifically addressed in this study. Troglitazone, another hepatotoxic compound and known BSEP substrate, caused a concentration dependent increase in intracellular fluorescence values, and a concurrent decrease in the supernatant - a similar scenario as seen for cyclosporine A (Fig. 4B). However, the dramatic decrease in fluorescence values observed at the highest tested concentration of troglitazone (100 μM) was due to cytotoxicity as evidenced by the CTB test. In contrast, the non-hepatotoxic compounds, chlorpheniramine and theophylline (both known not to inhibit BSEP or MRP2) did not cause any statistically significant increase in fluorescence inside the cells nor a decrease in the supernatant (Fig. 4B). The decrease in intracellular fluorescence observed for the three highest concentrations of chlorpheniramine is probably due to cytotoxicity.

Since the increase in fluorescence in cells and the decrease in the supernatant did not just mirror each other (Supplement 3), we investigated the outcome of combining both parameters. This can be achieved by fitting models to the fluorescence values for all concentrations in cells and in the supernatant, followed by calculating the difference between the models (cell *minus* supernatant), thus resulting in the 'model-difference' (Fig. 4B). Alternatively, it is possible to first subtract the fluorescence value of the supernatant from the fluorescence in the cells for each concentration and then fit a model to the difference, resulting in a so-called 'data-difference' curve (Fig. 4B). Thus, direct measurement and data modeling resulted in four parameters to describe export carrier inhibition (1. cell, 2. supernatant, 3. model-difference, and 4. data-difference, with the latter two being relatively similar). Subsequent experiments were then done to determine which of the four parameters best differentiates hepatotoxic and non-hepatotoxic compounds. A test concentration was considered as positive for any of the four above

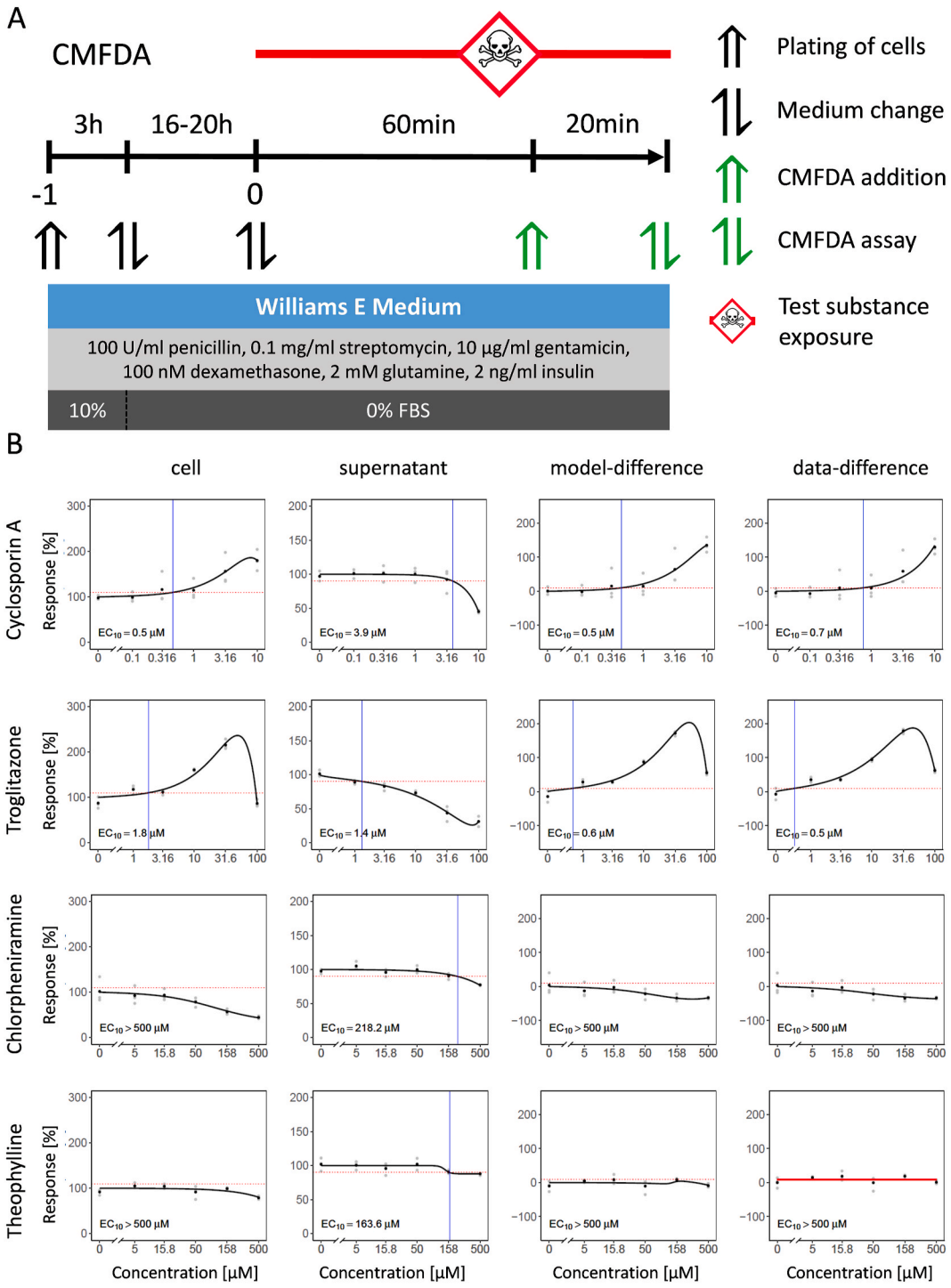

Fig. 4. Experimental schedule (A) and results of the CMFDA assay of four test compounds (B). Grey dots represent the results of three technical replicates, black dots denote the concentration-wise mean. Data of all compounds (n = 36) are given in Supplement 7 (curves) and 3 (data). The vertical blue lines indicate the EC_{10}. The bold red line indicates a flat profile (see methods).

mentioned parameters if the fitted curve exceeded the controls by 10% (EC_{10}) with exception of the supernatant where the fitted curve had to fall below the control by 10% (EC_{10}) (Table 1; Supplement 3).

3.5. Analysis of test compounds by the CTB assay

Reduced mitochondrial function that usually correlates with cytotoxicity was tested by the CTB-assay (Fig. 5A), where primary human hepatocytes were cultured under the same conditions as for the CMFDA assay, analyzing at least three donors per compound. The same test compounds are illustrated in Fig. 5B as for the CMFDA assay (Fig. 4B), with data from all others summarized in Supplement 9. The comparison of the CTB (Fig. 5B) and the CMFDA (Fig. 4B) assays show that cyclosporine A and troglitazone inhibited export carriers at non-cytotoxic concentrations; whereas, non-cytotoxic concentrations of chlorpheniramine and theophylline did not block the export of 5-CMF.

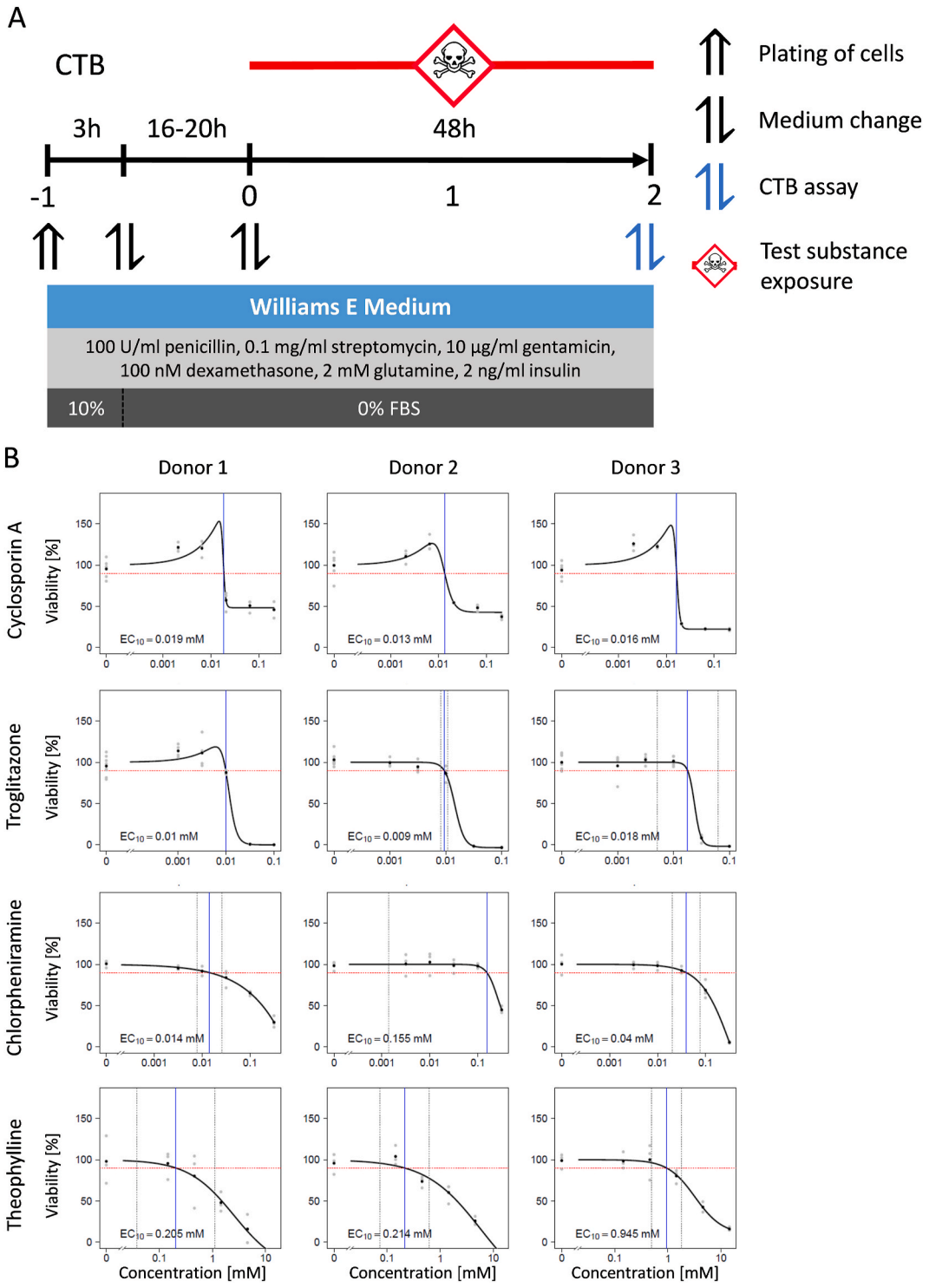

Fig. 5. Experimental schedule (A) and examples of the results of the CTB test (B). Grey dots represent the results of three to four technical replicates, black dots denote the concentration-wise mean and the data of all compounds and donors are documented in Supplement 3 (data) and 9 (curves). The vertical blue lines indicate the EC_{10}.

3.6. Differentiation of hepatotoxic compounds based on the CMFDA assay and CTB test

To compare the performance of our in vitro test system when using export carrier inhibition (CMFDA assay) as an endpoint to the CTB test - or a combination of both - we calculated the TSI, a measure of how well hepatotoxic and non-hepatotoxic compounds can be differentiated for a given set of compounds, and TEI, which informs how well a hepatotoxic C_{max} in vivo can be determined for these three options. Determining the EC_{10} based on the CTB assay alone led to a TSI of 0.775 and a TEI of 0.692 (Table 2A). The CMFDA assay resulted in a consistently higher TSI and TEI compared to the CTB test, regardless of whether the intra- or extracellular fluorescence values or the modelling-based results were used. The best performance (highest TSI and TEI) was achieved using the 'model-difference' for CMFDA (Table 2A). Next, the data of the CTB and the CMFDA assay were combined so that the lower EC_{10} of the respective

Table 2
Toxicity separation index (TSI) and toxicity estimation index (TEI) for the CTB and CMFDA assays alone and in combination.

A. TSI and TEI based on the EC_{10} values of the CTB and/or CMFDA assay and median values of three donors.

Assay	EC_{10} median	TSI	TEI
CTB	–	0.775	0.692
CMFDA	cell	0.863	0.729
	supernatant	0.801	0.747
	data-difference	0.865	0.762
	model-difference	0.889	0.798
Combination	CTB & cell	0.839	0.784
	CTB & supernatant	0.833	0.810
	CTB & data-difference	0.860	0.804
	CTB & model-difference	0.886	0.834

B. TSI and TEI for all possible parameter combinations considering EC_{10}, EC_{20}, …, EC_{90} as well as median, minimum (min) and maximum (max) values. The parameters resulting in the highest TSI are given for both assays alone and in combination. For a detailed list of the TSI and TEI values of all possible combinations see Supplement 3.

	TSI	TEI
CTB/EC_{20} max	0.842	0.637
CMFDA/EC_{10} min model-difference	0.915	0.874
CTB/EC_{20} max	0.933	0.873
CMFDA/EC_{10} min model-difference		
CTB/EC_{40} max	0.936	0.871
CMFDA/EC_{10} min model-difference		

assay was used. The combination of the CTB and CMFDA assay resulted in a higher TSI and TEI compared to the CTB assay alone (Table 2A). The in vitro - in vivo extrapolation plots of the CTB (Fig. 6A), CMFDA (Fig. 6B) and combined CTB-CMFDA data (Fig. 6C) illustrate that considering export kinetics in addition to the CTB test allows for a better differentiation of hepatotoxic and non-hepatotoxic compounds in relation to the maximal plasma concentration compared to using the CTB test alone.

To determine if the CTB or the CMFDA assay is more sensitive, we calculated $\log_2$ ratios of the EC_{10} values obtained from each assay for each of the 36 tested compounds, using the 'model-difference' for the CMFDA assay (Fig. 6D). A $\log_2$ ratio above zero indicates that the CMFDA assay is more sensitive. Interestingly, 14 of the tested compounds had a $\log_2$ ratio higher than two, while six compounds had ratios even higher than five, revealing that for these compounds the CMFDA assay was more sensitive. Conversely, the CMFDA assay was negative up to the highest tested concentration for 19 compounds, which was not surprising since no inhibition of export carriers was reported for the set of non-hepatotoxic substances.

For the analyses in Table 2A, we used the EC_{10} and median values, since these two parameters were previously shown to be optimal for a set of different compounds, where the TSI and TEI were calculated based on the CTB test [4]. However, in addition to the EC_{10}, all EC values between 10 and 90 could be used. Moreover, the minimum or maximum of the three donors may be used instead of the median to calculate the metrics. When we tested all possible combinations of EC_{10} to EC_{90} for the minimum, median and maximum, the highest TSI was obtained when CTB, EC_{40}, maximum was combined with the CMFDA assay, EC_{10}, minimum (Table 2B). This resulted in an even further improvement of the TSI to 0.936 and TEI to 0.871 (all possible combinations are given in Supplement 3). These very high metrics must be interpreted with caution due to overfitting. However, for future studies, it should be considered that parameters other than the EC_{10} and the median may be optimal when test batteries with several readouts are established.

3.7. Prediction of export inhibition using classification models

Finally, we investigated whether it was necessary to test all compounds with the CMFDA assay for export inhibition, or if it is possible to identify a subset of compounds with a high probability of a negative experimental result using an in silico method. Recently, a web service including classification models of different transporters was established that allows for the prediction of whether small molecules inhibit export carriers of hepatocytes [16]. In the present study, the web service was used to predict the inhibitory capacity of all test compounds (Supplement 10). Using these classification models on our set of selected compounds, a good agreement with the experimental data was obtained. If a score $\geq$0.65 [16] is used for the three carriers (BSEP, MRP3 and MRP4), 21 of the 36 compounds were predicted as positive. Experimentally, 17 out of the 36 compounds were positive in the CMFDA assay (Fig. 6D). If one considers the result of the export assay (CMFDA assay) as true positives or negatives, the classification resulted in a sensitivity, specificity, accuracy, negative prediction value (NPV) and positive prediction value (PPV) of 0.86, 0.85, 0.85, 0.92 and 0.75, respectively. Thus, the here-applied web service may indeed contribute towards reducing experimental effort in the future once the performance metrics presented here are confirmed with higher numbers of test compounds.

4. Discussion

Recently, we established a technique that allows for the determination of hepatotoxicity in relation to oral doses and blood concentrations [4] based solely on CTB test results generated in cultured human hepatocytes as the single in vitro readout. In the present study, we investigated whether we can improve the differentiation of hepatotoxic from non-hepatotoxic compounds, as evaluated by the TSI, by including inhibition of export carriers as a further in vitro readout in addition to the CTB test. Therefore, we established an assay that quantifies the ability of test compounds to inhibit the export of 5-CMF from human hepatocytes. Our results reveal that integration of this inhibition assay with the CTB test indeed allowed for a better separation of hepatotoxic and non-hepatotoxic compounds quantified by the TSI. Moreover, it also improved the estimation of hepatotoxic blood concentrations by the TEI.

The fluorophore 5-CMF is a substrate of several carriers, including BSEP and MRP2 [10]; therefore, delayed clearance of 5-CMF-associated fluorescence from hepatocytes after exposure to a test compound indicates inhibition of these export carriers (Fig. 1A). In drug induced cholestatic liver disease, bile acids accumulate in hepatocytes when their excretion is inhibited, leading to cytotoxicity [9]. Therefore, it was previously unclear if it is sufficient to use cytotoxicity or mitochondrial function tests as an in vitro readout for DILI analysis, or if inhibition of export carriers as an additional assay was of advantage. One reason that supports conducting both assays arises from the differences in the exposure of hepatocytes to bile acids in vitro and in vivo. In vivo, hepatocytes are constantly exposed to bile acids that are absorbed from the intestine and drained into the liver via the blood of the portal vein [2,30]. Moreover, cultured hepatocytes express low levels of Cyp7A1, a key enzyme of bile acid synthesis [26]. Therefore, bile acid accumulation due to export inhibition may result in less toxicity in cultured hepatocytes than in hepatocytes in vivo. However, the here-introduced CMFDA assay quantifies the inhibition of 5-CMF secretion, and thus an accumulation of bile acids up to cytotoxic levels due to this export inhibition is not required. Therefore, the results of the CMFDA assay will not be compromised if bile acid homeostasis of the cultured hepatocytes deviates from the in vivo situation, because the export inhibiting concentrations of the test compounds are based on an exogenously administered fluorophore.

An alternative approach would be to add bile acids to the culture medium to compensate for the decreased synthesis and exposure via the portal bloodstream. Importantly, this approach has already been performed [31,32], but not yet analyzed if it improves the differentiation of hepatotoxic and non-hepatotoxic compounds based on quantitative metrics. A further alternative to the here-established export assay is a technique based on artificial membrane vesicles that contain proteins, e.g. BSEP. This assay has been reported to detect BSEP inhibition at relatively low concentrations [33]. For example, an inhibitory

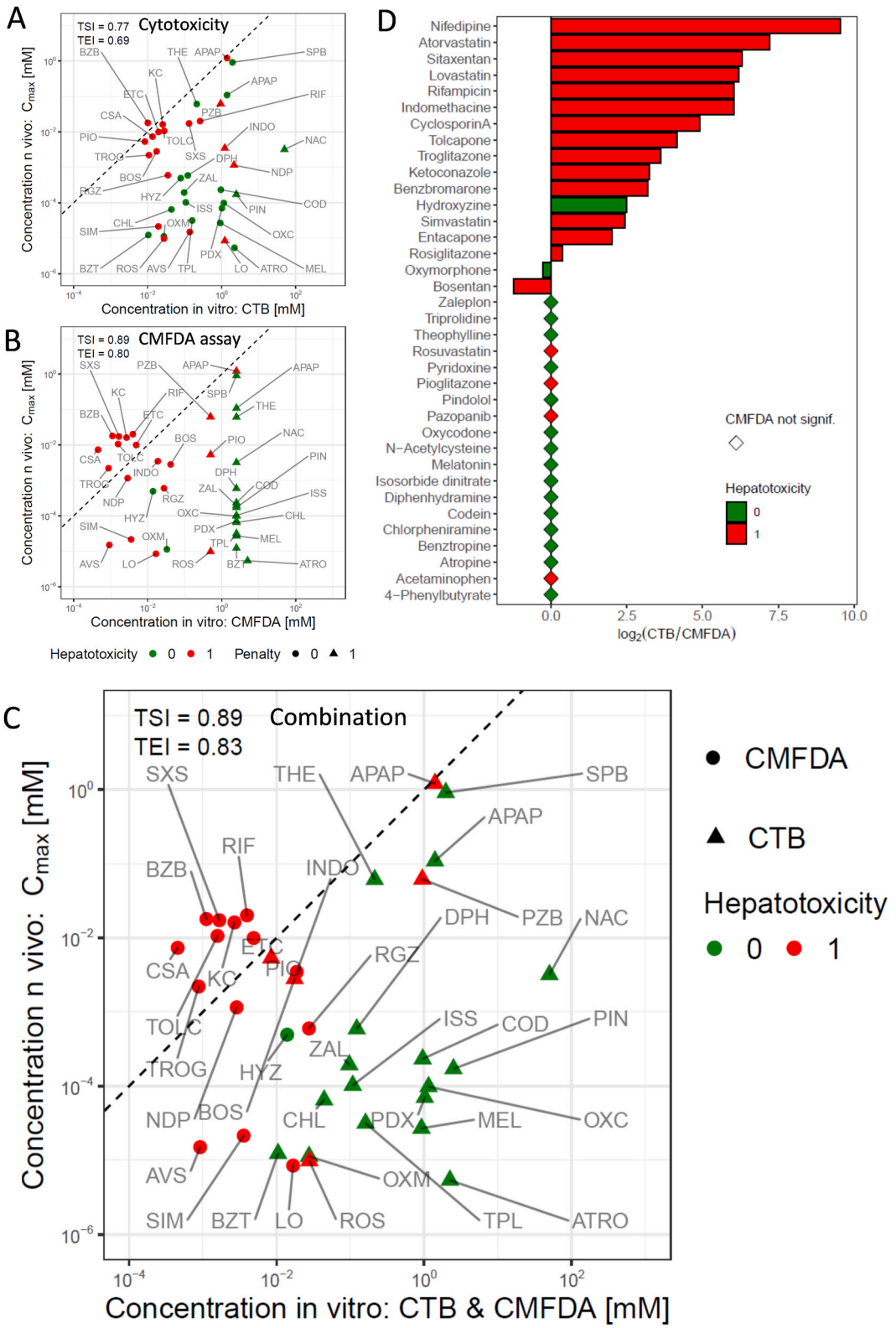

Fig. 6. The fluorescence export assay improves the differentiation of hepatotoxic from non-hepatotoxic compounds. Extrapolation plots **(A)** based on CTB test data alone using the EC_{10} median values (x-axis) and the C_{max} (total concentration in blood; 95%-CI); **(B)** based on the export assay (CMFDA assay using model-differences). For some compounds the CTB test (A) or the CMFDA assay (B) did not result in any positive results up to the highest soluble concentrations. These compounds are indicated by triangles (penalty: see methods). **(C)** based on the lower value of either the CTB test (triangle) or the CMFDA assay (circle) (x-axis). **(D)** Ratio plot comparing the CTB test and fluorescein export inhibition. Ratios were calculated by dividing the EC_{10} (median) values measured with the CTB assay by those obtained with the CMFDA assay and $\log_2$ values of the respective ratios are shown. 1: hepatotoxic; 0: non-hepatotoxic compounds. The dotted lines in A-C are iso-concentration lines that indicate identical concentrations for the x- and y-axes. The red and green symbols represent known hepatotoxic and non-hepatotoxic compounds in patients. Only APAP is included by two symbols, since hepatotoxic (red) and non-hepatotoxic (green) doses and blood concentrations are known (see Table 1).

concentration (IC_{50}) of 0.5 μM for BSEP and 14.5 μM for MRP2 was reported for cyclosporine A (Morgan et al., 2013). These values are similar to those obtained by the CMFDA assay in the present study (0.6 μM). An advantage of the vesicle assay is that it provides specific information, which carrier is inhibited, which is not easily possible by the hepatocyte export assay, since CMFDA/5-CMF in addition to being a substrate for the canalicular exporters MRP2 and BSEP, also appear to be transported by BCRP and MDR1/P-GP [34]. This does not invalidate the concept of the CMFDA assay but complicates the mechanistic explanation of toxicity for a certain compound if non bile acid efflux transporters are involved. For example, entacapone may be a more potent inhibitor of BCRP [35] than BSEP. On the other hand, the present CMFDA assay is performed in human hepatocytes with drug metabolizing capacity that would not be provided by the vesicle assay. Thus, future work should compare the here-established CMFDA assay to the vesicle assay and to assays with bile acid supplemented culture media with respect to the TSI and TEI in the same set of compounds.

An important aspect in test development is the choice of adequate culture conditions. First, we asked, if mouse hepatocytes cultured as a spheroid or as a sheet of cells are more suitable (Fig. 2). Because of the reproducible kinetics we decided to continue with hepatocytes cultured as sheets, either as sandwich or monolayer cultures; in contrast, individual cells in the spheroids showed a high degree of variability which was not observed in vivo. It has been reported that SC may allow for better long-term maintenance of differentiated hepatocellular functions than conventional cell cultures, but on the other hand, they also require greater experimental effort [2]. Our results do not indicate that the sandwich culture of human hepatocytes has any advantage over the monolayer culture with respect to export kinetics. This may be due to the fact that the here-established method represents a short-term assay with only 1 h of test compound incubation followed by 20 min of substrate (CMFDA) exposure. Further advantages of the monolayer culture include the rapid and homogeneous uptake of CMFDA into all cultured hepatocytes, the reproducible export kinetics, and that the technique is easy to standardize (Supplement 2).

To minimize the experimental workload, we investigated if it was necessary to test all compounds in the CMFDA assay for export inhibition, or if we could use an in silico method to identify a subset of compounds with a high probability of a negative experimental result, so that these negatively predicted compounds would not require testing with the CMFDA assay. The here-applied machine learning approach for BSEP, MRP3 and MRP4 inhibition [16] identified 16 of 17 compounds that inhibited 5-CMF export in hepatocytes. Thus, the in silico technique may indeed reduce the experimentally required effort, but a higher number of substances must be studied before a recommendation for routine application is possible. Furthermore, the addition of MRP2 inhibition, for which there is currently no model available, could improve the prediction. Compounds identified as export inhibitors (or competitive for 5-CMF export) by the in silico tool still require experimental testing, because the EC_{10} cannot be obtained in silico.

A limitation of the established CMFDA assay is that the set of tested hepatotoxic compounds consisted mostly of known BSEP and/or MRP2 inhibitors or substrates. Although, the analysis of 'gold standard compounds' represents an essential first step in test system development [1], the method must next be tested on a large, representative set of hepatotoxic and non-hepatotoxic compounds. Our selection of hepatotoxic compounds that act as export carrier inhibitors (including competitive substrates) may also explain the very high TSI based on the CMFDA assay alone. Such a high TSI may decrease in a representative set of hepatotoxic compounds for which mechanisms other than export inhibition are relevant. However, good separation may still be possible by including cytotoxicity assays, and eventually functional tests, e.g. lipid accumulation or cytokine release.

The Biopharmaceutics Drug Disposition Classification System (BDDCS) was developed that differentiates four classes of compounds based on their solubility and permeability [36]. This system also considers the observation that highly permeable substances are often extensively metabolized and this property is associated with a higher risk of developing DILI [37]. BDDCS Class 2 compounds with a low solubility and high permeability are known to be associated with a high DILI risk [37,38]. For DILI prediction the BDDCS class may additionally be combined with the dose (e.g., dose $\geq$50 mg). It has been published that measures of BSEP inhibition do not improve DILI prediction but rather most potent BSEP inhibitors (including competitive inhibitors) are BDDCS Class 2 drugs [39]. In future, it will be important to study if readouts from in vitro tests e.g., cytotoxicity, carrier inhibition, gene expression alterations, reactive metabolite formation etc. will improve DILI prediction independent from BDDCS Class. For this purpose, large sets of compounds (>100) with sufficient substances from all four BDDCS will be required.

In conclusion, a short-term in vitro test has been established that allows for the detection of bile acid export carrier inhibition in cultured human hepatocytes. When used in combination with the CTB test, this method improves the identification of DILI compounds compared to mitochondrial function/cytotoxicity analysis alone in a set of compounds where export carrier inhibition is relevant for hepatotoxicity.

Funding statement

This work has been supported in part by the Research Training Group "Biostatistical Methods for High-Dimensional Data in Toxicology" (RTG 2624, Project P1 and P2) funded by the Deutsche Forschungsgemeinschaft (DFG, German Research Foundation - Project Number 427806116). Furthermore, this work has received funding from the European Union's Horizon 2020 research and innovation programme under grant agreement no. 681002 (EU-ToxRisk) and LivSysTransfer (BMBF, 031L0119).

Author statement

T.B.: Conceptualization, Data curation, Formal analysis, Validation, Visualization, Writing - original draft, Writing - review & editing, Investigation. W.A.: Conceptualization, Data curation, Formal analysis, Validation, Investigation. F.K.: Data curation, Formal analysis, Validation, Visualization.J.D.: Data curation, Formal analysis, Validation, Visualization. N.V.: Conceptualization, Supervision. K.E.: Conceptualization, Writing - review & editing. R.M.: Conceptualization, Writing - review & editing. A.G.: Investigation, Formal analysis, Visualization. C. C.: Conceptualization, Writing - review & editing. G.G.: Investigation, Formal analysis, Visualization. M.L.: Conceptualization, Writing - review & editing. M.Z.: Data curation, Formal analysis, Software. I.G.: Data curation, Formal analysis, Software. J.R.: Data curation, Formal analysis, Investigation. F.G.M.R.: Conceptualization, Writing - review & editing. A.J.F.: Conceptualization, Resources. D.P.W.: Conceptualization, Resources.A.D-V.: Conceptualization, Supervision. M.G.: Data curation, Formal analysis. G.E.: Data curation, Formal analysis. N.K.: Conceptualization, Writing - review & editing. J.R.: Conceptualization, Writing - review & editing, Supervision.J.G.H.: Conceptualization, Funding acquisition, Project administration, Supervision, Writing - original draft, Writing - review & editing.

Declaration of competing interest

The authors declare that they have no known competing financial interests or personal relationships that could have appeared to influence the work reported in this paper.

Appendix A. Supplementary data

Supplementary data to this article can be found online at https://doi.org/10.1016/j.cbi.2021.109728.

References

[1] A. Sachinidis, W. Albrecht, P. Nell, A. Cherianidou, N.J. Hewitt, K. Edlund, J. G. Hengstler, Road map for development of stem cell-based alternative test methods, Trends Mol. Med. 25 (2019) 470–481, https://doi.org/10.1016/j.molmed.2019.04.003.

[2] P. Godoy, N.J. Hewitt, U. Albrecht, M.E. Andersen, N. Ansari, S. Bhattacharya, J. G. Bode, J. Bolleyn, C. Borner, J. Böttger, A. Braeuning, R.A. Budinsky, B. Burkhardt, N.R. Cameron, G. Camussi, C.S. Cho, Y.J. Choi, J. Craig Rowlands, U. Dahmen, G. Damm, O. Dirsch, M.T. Donato, J. Dong, S. Dooley, D. Drasdo, R. Eakins, K.S. Ferreira, V. Fonsato, J. Fraczek, R. Gebhardt, A. Gibson, M. Glanemann, C.E.P. Goldring, M.J. Gómez-Lechón, G.M.M. Groothuis, L. Gustavsson, C. Guyot, D. Hallifax, S. Hammad, A. Hayward, D. Häussinger, C. Hellerbrand, P. Hewitt, S. Hoehme, H.G. Holzhütter, J.B. Houston, J. Hrach, K. Ito, H. Jaeschke, V. Keitel, J.M. Kelm, B. Kevin Park, C. Kordes, G.A. Kullak-Ublick, E.L. Lecluyse, P. Lu, J. Luebke-Wheeler, A. Lutz, D.J. Maltman, M. Matz-Soja, P. McMullen, I. Merfort, S. Messner, C. Meyer, J. Mwinyi, D.J. Naisbitt, A. K. Nussler, P. Olinga, F. Pampaloni, J. Pi, L. Pluta, S.A. Przyborski, A. Ramachandran, V. Rogiers, C. Rowe, C. Schelcher, K. Schmich, M. Schwarz, B. Singh, E.H.K. Stelzer, B. Stieger, R. Stöber, Y. Sugiyama, C. Tetta, W.E. Thasler, T. Vanhaecke, M. Vinken, T.S. Weiss, A. Widera, C.G. Woods, J.J. Xu, K. M. Yarborough, J.G. Hengstler, Recent advances in 2D and 3D in vitro systems using primary hepatocytes, alternative hepatocyte sources and non-parenchymal liver cells and their use in investigating mechanisms of hepatotoxicity, cell signaling and ADME, Arch. Toxicol. 87 (2013) 1315–1530, https://doi.org/10.1007/s00204-013-1078-5.

[3] N.J. Hewitt, M.J.G. Lechón, J.B. Houston, D. Hallifax, H.S. Brown, P. Maurel, J. G. Kenna, L. Gustavsson, C. Lohmann, C. Skonberg, A. Guillouzo, G. Tuschl, A.P. Li, E. Lecluyse, G.M.M. Groothuis, J.G. Hengstler, Primary hepatocytes: current understanding of the regulation of metabolic enzymes and transporter proteins, and pharmaceutical practice for the use of hepatocytes in metabolism, enzyme induction, transporter, clearance, and hepatotoxicity studies, Drug Metab. Rev. 39 (2007) 159–234, https://doi.org/10.1080/03602530601093489.

[4] W. Albrecht, F. Kappenberg, T. Brecklinghaus, R. Stoeber, R. Marchan, M. Zhang, K. Ebbert, H. Kirschner, M. Grinberg, M. Leist, W. Moritz, C. Cadenas, A. Ghallab, J. Reinders, N. Vartak, C. van Thriel, K. Golka, L. Tolosa, J.V. Castell, G. Damm, D. Seehofer, A. Lampen, A. Braeuning, T. Buhrke, A.C. Behr, A. Oberemm, X. Gu, N. Kittana, B. van de Water, R. Kreiling, S. Fayyaz, L. van Aerts, B. Smedsrød, H. Ellinger-Ziegelbauer, T. Steger-Hartmann, U. Gundert-Remy, A. Zeigerer, A. Ullrich, D. Runge, S.M.L. Lee, T.S. Schiergens, L. Kuepfer, A. Aguayo-Orozco, A. Sachinidis, K. Edlund, I. Gardner, J. Rahnenführer, J.G. Hengstler, Prediction of human drug-induced liver injury (DILI) in relation to oral doses and blood concentrations, Arch. Toxicol. 93 (2019) 1609–1637, https://doi.org/10.1007/s00204-019-02492-9.

[5] M. Leist, A. Ghallab, R. Graepel, R. Marchan, R. Hassan, S.H. Bennekou, A. Limonciel, M. Vinken, S. Schildknecht, T. Waldmann, E. Danen, B. van Ravenzwaay, H. Kamp, I. Gardner, P. Godoy, F.Y. Bois, A. Braeuning, R. Reif, F. Oesch, D. Drasdo, S. Höhme, M. Schwarz, T. Hartung, T. Braunbeck, J. Beltman, H. Vrieling, F. Sanz, A. Forsby, D. Gadaleta, C. Fisher, J. Kelm, D. Fluri, G. Ecker, B. Zdrazil, A. Terron, P. Jennings, B. van der Burg, S. Dooley, A.H. Meijer, E. Willighagen, M. Martens, C. Evelo, E. Mombelli, O. Taboureau, A. Mantovani, B. Hardy, B. Koch, S. Escher, C. van Thriel, C. Cadenas, D. Kroese, B. van de Water, J.G. Hengstler, Adverse outcome pathways: opportunities, limitations and open questions, Arch. Toxicol. 91 (2017) 3477–3505, https://doi.org/10.1007/s00204-017-2045-3.

[6] A. Ghallab, U. Hofmann, S. Sezgin, N. Vartak, R. Hassan, A. Zaza, P. Godoy, K. M. Schneider, G. Guenther, Y.A. Ahmed, A.A. Abbas, V. Keitel, L. Kuepfer, S. Dooley, F. Lammert, C. Trautwein, M. Spiteller, D. Drasdo, A.F. Hofmann, P.L. M. Jansen, J.G. Hengstler, R. Reif, Bile microinfarcts in cholestasis are initiated by rupture of the apical hepatocyte membrane and cause shunting of bile to sinusoidal blood, Hepatology 69 (2019) 666–683, https://doi.org/10.1002/hep.30213.

[7] W.R. Proctor, A.J. Foster, J. Vogt, C. Summers, B. Middleton, M.A. Pilling, D. Shienson, M. Kijanska, S. Ströbel, J.M. Kelm, P. Morgan, S. Messner, D. Williams, Utility of spherical human liver microtissues for prediction of clinical drug-induced liver injury, Arch. Toxicol. 91 (2017) 2849–2863, https://doi.org/10.1007/s00204-017-2002-1.

[8] K. Gianmoena, N. Gasparoni, A. Jashari, P. Gabrys, K. Grgas, A. Ghallab, K. Nordström, G. Gasparoni, J. Reinders, K. Edlund, P. Godoy, A. Schriewer, H. Hayen, C.A. Hudert, G. Damm, D. Seehofer, T.S. Weiss, P. Boor, H.-J. Anders, M. Motrapu, P. Jansen, T.S. Schiergens, M. Falk-Paulsen, P. Rosenstiel, C. Lisowski, E. Salido, R. Marchan, J. Walter, J.G. Hengstler, C. Cadenas, Epigenomic and transcriptional profiling identifies impaired glyoxylate detoxification in NAFLD as a risk factor for hyperoxaluria, Cell Rep. 36 (2021) 109526, https://doi.org/10.1016/j.celrep.2021.109526.

[9] P.L.M. Jansen, A. Ghallab, N. Vartak, R. Reif, F.G. Schaap, J. Hampe, J. G. Hengstler, The ascending pathophysiology of cholestatic liver disease, Hepatology 65 (2017) 722–738, https://doi.org/10.1002/hep.28965.

[10] L. Qiu, J. Finley, M. Taimi, M.D. Aleo, C. Strock, J. Gilbert, S. Qin, Y. Will, High-content imaging in human and rat hepatocytes using the fluorescent dyes CLF and CMFDA is not specific enough to assess BSEP/bsep and/or MRP2/mrp2 inhibition by cholestatic drugs, Appl. Vitr. Toxicol. 1 (2015) 198–212, https://doi.org/10.1089/aivt.2015.0014.

[11] X. Gu, W. Albrecht, K. Edlund, F. Kappenberg, J. Rahnenführer, M. Leist, W. Moritz, P. Godoy, C. Cadenas, R. Marchan, T. Brecklinghaus, L.T. Pardo, J. V. Castell, I. Gardner, B. Han, J.G. Hengstler, R. Stoeber, Relevance of the incubation period in cytotoxicity testing with primary human hepatocytes, Arch. Toxicol. 92 (2018) 3505–3515, https://doi.org/10.1007/s00204-018-2302-0.

[12] O. Frey, P.M. Misun, D.A. Fluri, J.G. Hengstler, A. Hierlemann, Reconfigurable microfluidic hanging drop network for multi-tissue interaction and analysis, Nat. Commun. 5 (2014) 1–11, https://doi.org/10.1038/ncomms5250.

[13] R. Reif, A. Ghallab, L. Beattie, G. Günther, L. Kuepfer, P.M. Kaye, J.G. Hengstler, In vivo imaging of systemic transport and elimination of xenobiotics and endogenous molecules in mice, Arch. Toxicol. 91 (2017) 1335–1352, https://doi.org/10.1007/s00204-016-1906-5.

[14] L.S. New, E.C.Y. Chan, Evaluation of BEH C18, BEH HILIC, and HSS T3 (C18) column chemistries for the UPLC-MS-MS analysis of glutathione, glutathione disulfide, and ophthalmic acid in mouse liver and human plasma, J. Chromatogr. Sci. 46 (2008) 209–214, https://doi.org/10.1093/chromsci/46.3.209.

[15] B. MacLean, D.M. Tomazela, N. Shulman, M. Chambers, G.L. Finney, B. Frewen, R. Kern, D.L. Tabb, D.C. Liebler, M.J. MacCoss, Skyline: an open source document editor for creating and analyzing targeted proteomics experiments, Bioinformatics 26 (2010) 966–968, https://doi.org/10.1093/bioinformatics/btq054.

[16] F. Montanari, B. Knasmüller, S. Kohlbacher, C. Hillisch, C. Baierová, M. Grandits, G.F. Ecker, Vienna LiverTox workspace—a set of machine learning models for prediction of interactions profiles of small molecules with transporters relevant for regulatory agencies, Front. Chem. 7 (2020) 899, https://doi.org/10.3389/fchem.2019.00899.

[17] S. Köppert, A. Büscher, A. Babler, A. Ghallab, E.M. Buhl, E. Latz, J.G. Hengstler, E. R. Smith, W. Jahnen-Dechent, Cellular clearance and biological activity of calciprotein particles depend on their maturation state and crystallinity, Front. Immunol. 9 (2018) 1991, https://doi.org/10.3389/fimmu.2018.01991.

[18] A. Wilson, N. Norden, The R Project for statistical computing the R Project for statistical computing, URL Http//Www. r-Project. Org/254, https://www.r-project.org/, 2015. (Accessed 10 May 2021). accessed,3,1,9.

[19] (n.d Cran - Package DoseFinding. https://cran.r-project.org/web/packages/DoseFinding/index.html. (Accessed 10 May 2021) accessed.

[20] C. Ritz, F. Baty, J.C. Streibig, D. Gerhard, Dose-response analysis using R, PLoS One 10 (2015), e0146021, https://doi.org/10.1371/journal.pone.0146021.

[21] X. Robin, N. Turck, A. Hainard, N. Tiberti, F. Lisacek, J.C. Sanchez, M. Müller, pROC: an open-source package for R and S+ to analyze and compare ROC curves, BMC Bioinf. 12 (2011) 1–8, https://doi.org/10.1186/1471-2105-12-77.

[22] F. Kappenberg, T. Brecklinghaus, W. Albrecht, J. Blum, C. van der Wurp, M. Leist, J.G. Hengstler, J. Rahnenführer, Handling deviating control values in concentration-response curves, Arch. Toxicol. 94 (2020) 3787–3798, https://doi.org/10.1007/s00204-020-02913-0.

[23] P. Brain, R. Cousens, An equation to describe dose responses where there is stimulation of growth at low doses, Weed Res. 29 (1989) 93–96, https://doi.org/10.1111/j.1365-3180.1989.tb00845.x.

[24] H. Akaike, Akaike's information criterion, in: Int. Encycl. Stat. Sci., Springer Berlin Heidelberg, 2011, https://doi.org/10.1007/978-3-642-04898-2_110, 25–25.

[25] F. Bretz, J.C. Pinheiro, M. Branson, Combining multiple comparisons and modeling techniques in dose-response studies, Biometrics 61 (2005) 738–748, https://doi.org/10.1111/j.1541-0420.2005.00344.x.

[26] P. Godoy, A. Widera, W. Schmidt-Heck, G. Campos, C. Meyer, C. Cadenas, R. Reif, R. Stöber, S. Hammad, L. Pütter, K. Gianmoena, R. Marchan, A. Ghallab, K. Edlund, A. Nüssler, W.E. Thasler, G. Damm, D. Seehofer, T.S. Weiss, O. Dirsch, U. Dahmen, R. Gebhardt, U. Chaudhari, K. Meganathan, A. Sachinidis, J. Kelm, U. Hofmann, R. P. Zahedi, R. Guthke, N. Blüthgen, S. Dooley, J.G. Hengstler, Gene network activity in cultivated primary hepatocytes is highly similar to diseased mammalian liver tissue, Arch. Toxicol. 90 (2016) 2513–2529, https://doi.org/10.1007/s00204-016-1761-4.

[27] G. Campos, W. Schmidt-Heck, J. De Smedt, A. Widera, A. Ghallab, L. Pütter, D. González, K. Edlund, C. Cadenas, R. Marchan, R. Guthke, C. Verfaillie, C. Hetz, A. Sachinidis, A. Braeuning, M. Schwarz, T.S. Weiß, B.K. Banhart, J. Hoek, R. Vadigepalli, J. Willy, J.L. Stevens, D.C. Hay, J.G. Hengstler, P. Godoy, Inflammation-associated suppression of metabolic gene networks in acute and chronic liver disease, Arch. Toxicol. 94 (2020) 205–217, https://doi.org/10.1007/s00204-019-02630-3.

[28] F.J. Romero, H. Sies, Subcellular glutathione contents in isolated hepatocytes treated with L-buthionine sulfoximine, Biochem. Biophys. Res. Commun. 123 (1984) 1116–1121, https://doi.org/10.1016/S0006-291X(84)80248-X.

[29] R. Li, P. Zhang, C. Li, W. Yang, Y. Yin, K. Tao, Tert-butylhydroquinone mitigates carbon tetrachloride induced hepatic injury in mice, Int. J. Med. Sci. 17 (2020) 2095–2103, https://doi.org/10.7150/ijms.45842.

[30] N. Vartak, G. Guenther, F. Joly, A. Damle-Vartak, G. Wibbelt, J. Fickel, S. Jörs, B. Begher-Tibbe, A. Friebel, K. Wansing, A. Ghallab, M. Rosselin, N. Boissier, I. Vignon-Clementel, C. Hedberg, F. Geisler, H. Hofer, P. Jansen, S. Hoehme, D. Drasdo, J.G. Hengstler, Intravital dynamic and correlative imaging of mouse livers reveals diffusion-dominated canalicular and flow-augmented ductular bile flux, Hepatology 73 (2021) 1531–1550, https://doi.org/10.1002/hep.31422.

[31] S. Chatterjee, L. Richert, P. Augustijns, P. Annaert, Hepatocyte-based in vitro model for assessment of drug-induced cholestasis, Toxicol. Appl. Pharmacol. 274 (2014) 124–136, https://doi.org/10.1016/j.taap.2013.10.032.

[32] J.P. Jackson, K.M. Freeman, R.L. St Claire, C.B. Black, K.R. Brouwer, Cholestatic drug induced liver injury: a function of bile salt export pump inhibition and farnesoid X receptor antagonism, Appl. Vitr. Toxicol. 4 (2018) 265–279, https://doi.org/10.1089/aivt.2018.0011.

[33] R.E. Morgan, C.J. van Staden, Y. Chen, N. Kalyanaraman, J. Kalanzi, R.T. Dunn, C. A. Afshari, H.K. Hamadeh, A multifactorial approach to hepatobiliary transporter assessment enables improved therapeutic compound development, Toxicol. Sci. 136 (2013) 216–241, https://doi.org/10.1093/toxsci/kft176.

[34] P. Caetano-Pinto, M.J. Janssen, L. Gijzen, L. Verscheijden, M.J.G. Wilmer, R. Masereeuw, Fluorescence-based transport assays revisited in a human renal proximal tubule cell line, Mol. Pharm. 13 (2016) 933–944, https://doi.org/10.1021/acs.molpharmaceut.5b00821.

[35] J. Bicker, A. Fortuna, G. Alves, P. Soares-Da-Silva, A. Falcão, Elucidation of the impact of P-glycoprotein and breast cancer resistance protein on the brain distribution of catechol-O-methyltransferase inhibitors, Drug Metab. Dispos. 45 (2017) 1282–1291, https://doi.org/10.1124/dmd.117.077883.

[36] C.Y. Wu, L.Z. Benet, Predicting drug disposition via application of BCS: transport/absorption/elimination interplay and development of a biopharmaceutics drug disposition classification system, Pharm. Res. (N. Y.) 22 (2005) 11–23, https://doi.org/10.1007/s11095-004-9004-4.

[37] R. Chan, L.Z. Benet, Evaluation of DILI predictive hypotheses in early drug development, Chem. Res. Toxicol. 30 (2017) 1017–1029, https://doi.org/10.1021/acs.chemrestox.7b00025.

[38] R. Chan, L.Z. Benet, Evaluation of the relevance of DILI predictive hypotheses in early drug development: review of: in vitro methodologies vs. BDDCS classification, Toxicol. Res. (Camb). 7 (2018) 358–370, https://doi.org/10.1039/c8tx00016f.

[39] R. Chan, L.Z. Benet, Measures of BSEP inhibition in vitro are not useful predictors of DILI, Toxicol. Sci. 162 (2018) 499–508, https://doi.org/10.1093/toxsci/kfx284.